



21st European Conference on Fracture, ECF21, 20-24 June 2016, Catania, Italy

Stress corrosion cracking of gas pipeline steels of different strength

O. I. Zvirko ^{a*}, S. F. Savula ^b, V. M. Tsependa ^b, G. Gabetta ^c, H. M. Nykyforchyn ^a

^a *Karpenko Physico-Mechanical Institute of the National Academy of Sciences of Ukraine, 5, Naukova St., 79060 Lviv, Ukraine*

^b *Public Joint-Stock Company "UKRTRANSGAZ, Affiliate "Lvivtransgaz", 3, Rubchaka St., 79026 Lviv, Ukraine;*

^c *eni S.p.A., 1, Piazzale Mattei, 00144 Rome, Italy*

Abstract

With the development of the natural gas industry, gas transmission pipelines have been developed rapidly in terms of safety, economy and efficiency. Our recent studies have shown that an important factor of main pipelines serviceability loss under their long-term service is the in-bulk metal degradation of the pipe wall. This leads to the loss of the initial mechanical properties, primarily, resistance to brittle fracture, which were set in engineering calculations at the pipeline design stage. At the same time stress corrosion cracking has been identified as one of the predominant failures in pipeline steels in humid environments, which causes rupture of high-pressure gas transmission pipes as well as serious economic losses and disasters.

In the present work the low-carbon pipeline steels with different strength levels from the point of view of their susceptibility to stress corrosion cracking in the as-received state and after in-laboratory accelerated degradation under environmental conditions similar to those of an acidic soil were investigated. The main objectives of this study were to determine whether the development of higher strength materials led to greater susceptibility to stress corrosion cracking and whether degraded pipeline steels became more susceptible to stress corrosion cracking than in the as-received state. The procedure of accelerated degradation of pipeline steels was developed and introduced in laboratory under the combined action of axial loading and hydrogen charging. It proved to be reliable and useful to performed laboratory simulation of in-service degradation of pipeline steels with different strength. The in-laboratory degraded 17H1S and X60 pipeline steels tested in the NS4 solution saturated with CO₂ under open circuit potential revealed the susceptibility to stress corrosion cracking, reflected in the degradation of mechanical properties, and at the same time the degraded X60 steel showed higher resistance to stress corrosion cracking than the degraded 17H1S steel. Fractographic observation confirmed the pipeline steels hydrogen embrittlement caused by the permeated hydrogen.

Copyright © 2016 The Authors. Published by Elsevier B.V. This is an open access article under the CC BY-NC-ND license (<http://creativecommons.org/licenses/by-nc-nd/4.0/>).

Peer-review under responsibility of the Scientific Committee of ECF21.

Keywords: stress corrosion cracking; slow strain rate tests; mechanical properties; pipeline steel.

* Corresponding author. Tel.: +38032-229-6294; fax: +38032-264-9427.

E-mail address: zvi@ipm.lviv.ua, olha.zvirko@gmail.com (O. I. Zvirko)

1. Introduction

With the development of the natural gas industry, the gas transmission pipelines have been developed rapidly in terms of safety, economy and efficiency. It was demonstrated by Gabetta et al. (2008) and Nykyforchyn et al. (2010) that an important factor of main pipelines serviceability loss during their long-term service is the in-bulk metal degradation of the pipe wall. This leads to the loss of the designed initial mechanical properties, primarily, resistance to brittle fracture. The degradation processes of the main oil and gas pipelines steels are accelerated by severe operating conditions, such as long-term interaction of the stressed metal with corrosive-hydrogenated environment, cyclic pressure changes and temperature fluctuations.

At the same time stress corrosion cracking (SCC) has been identified as one of the predominant failures in pipeline steels in humid environments, which causes rupture of high-pressure gas transmission pipes as well as serious economic losses and disasters. SCC occurred on the external surface of the gas transmission pipelines in certain locations where they are subjected to coating disbonding, external damages, inherent mill defects, soil movements and third party damages. It is characterized by the initiation and propagation of cracks and takes place under the simultaneous action of tensile stresses and specific corrosive environment on a susceptible material.

The integrity of the underground low-alloyed pipeline steels used for gas transport depends greatly on soil environment composition. Thus near-neutral-pH SCC (also referred to as low-pH SCC) of pipelines are often revealed when predominantly located in poorly drained soils. The cracking environment appears to be a diluted groundwater containing dissolved CO_2 . The near-neutral-pH SCC has been extensively investigated by Elboujdaini et al. (2000), Lu et al. (2006), Bolzon et al. (2011) and others. Typically, SCC colonies are initiated at the external surface sites where there is already pitting or general corrosion (Fig. 1). The solution termed NS4 was developed to simulate SCC environments and it became the favoured standard environment for crack propagation testing in most laboratories. The peculiarity of our research was the use of NS4 solution (purged with CO_2 only) with a lower pH (pH5.7) instead of standard NS4 solution in order to estimate the impact of acid soils on SCC of the pipeline steels.

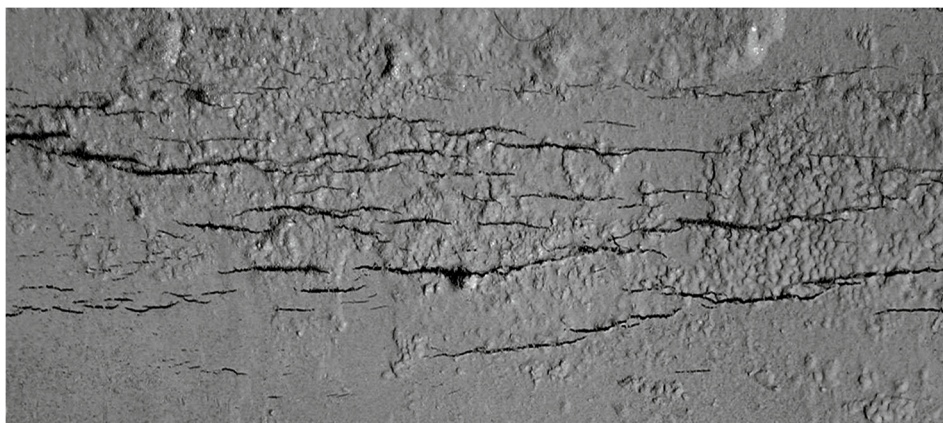


Fig. 1. Example of the colony of stress corrosion cracks on the external surface of the high-pressure gas transmission pipeline.

The principal question was to evaluate the possible effect of pipeline steel degradation on the increase of its susceptibility to SCC. Therefore, to find out the answer the accelerated degradation of pipelines steels in the laboratory under the combined action of axial loading and electrolytic hydrogenation was introduced in the study.

The purpose of the present work was to study the susceptibility to SCC of the pipeline steels of different strength levels in the as-received state and after their in-laboratory accelerated degradation under environmental conditions similar to those of a soil. For this purpose the NS4 simulated ground water solution with pH5.7 was used, involving electrochemical study and the slow strain rate testing (SSRT) techniques.

2. Objects, materials and methods

In this work the susceptibility of the main pipeline steels to SCC was investigated. Two 17H1S (Ukrainian code, equivalent to X52) and X60 low-alloyed pipeline steels were studied. The specimens were cut out the real pipes: 1) 17H1S steel pipe with outer diameter $D = 529$ mm and wall thickness $t = 8$ mm and 2) X60 steel pipe with outer diameter $D = 455$ mm and wall thickness $t = 14$ mm.

The characteristics of the as-received pipeline steels with different strength from the point of view of their SCC resistance were compared and then they were compared with the properties of pipeline steels after accelerated degradation too.

A series of specimens were tested:

- 1) in as-received state;
- 2) in degraded state after in-laboratory accelerated degradation. Accelerated degradation was performed with the use of the following parameters: the specimens were electrolytically hydrogen pre-charged in an aqueous sulphuric acid solution (pH2) at 20 mA/cm^2 for 95 hours before subjecting the specimens to an axial loading up to a value of the axial strain 2.8%; then they were exposed to artificial aging at 250°C for 1 hour. This applied procedure enabled, on a laboratory scale, simulating of the pipeline steel degradation during long-term exploitation under simultaneous action of hydrogenation and working loading.

The laboratory investigations were performed in a simulated soil solution NS4, representing the ground water found around SCC sites. Chemical composition of NS4 test solution, used for laboratory simulations is presented in Table 1. The test solution was prepared from analytical grade reagents. To estimate the impact of acid soils on SCC of pipeline steels and to achieve the lower pH value (pH5.7) NS4 solution was purged with CO_2 instead of 5% CO_2/N_2 mixture. Prior to each electrochemical and SSRT test, the solutions were purged with CO_2 gas for 1 hour. The gas flow was maintained throughout the test.

Table 1. Chemical composition of NS4 test solution.

Components	KCl	NaHCO_3	$\text{CaCl}_2 \cdot 2\text{H}_2\text{O}$	$\text{MgSO}_4 \cdot 7\text{H}_2\text{O}$
Concentration in g/L	0.122	0.483	0.181	0.131

The electrochemical tests were carried out on potentiostat IPC-Pro controlled with a computer, using a standard temperature-controlled electrochemical cell with typical three-electrode system consisting of the working electrode, Ag/AgCl (saturated KCl), reference electrode and Pt auxiliary electrode. The working electrodes were made from the studied steels in the form of bars 1.0×0.7 cm and length of 3 cm, all surfaces were polished. Insulating waterproof coating was applied on all surfaces of the working electrodes, except the selected area $\sim 0.5 \text{ cm}^2$ for electrochemical studies. Potentiodynamic polarization curves were obtained by sweeping the potential from -1.1 V to corrosion potential (E_{corr}) $E_{corr} + 0.4 \text{ V}$ vs. Ag/AgCl at a sweep rate of $1.0 \text{ mV} \cdot \text{s}^{-1}$. The basic electrochemical characteristics of steels (corrosion potential E_{corr} , corrosion current density i_{corr}) were determined by the graph-analytic method.

Susceptibility of the investigated steels to SCC was studied under specimen tension with slow rate of loading. Tests were performed under the open circuit condition (at corrosion potential E_{corr}). For the SSRT, smooth cylindrical tensile specimens with a 25 mm gauge length and 5 mm gauge diameter were machined from the low-alloyed pipeline steels in the longitudinal rolling direction. Before testing, the specimens were abraded longitudinally with a 600-grade emery paper and degreased. Specimens were subjected to monotonic SSRT at a strain rate of 10^{-6} s^{-1} . The tests were conducted under room temperature in air as an inert environment, and in NS4 test solution saturated with CO_2 . The results obtained from the SSRT in the corrosive environment were compared to those in air.

The steel plate specimens ($\sim 1 \text{ cm}^3$) were sliced and polished up to $1 \mu\text{m}$ diamond paste for the microstructure observation. After the last sequence of polishing, the specimens are rinsed with distilled water, cleaned with a cloth, rinsed again; flushed with ethanol and dried under warm air flow. This operation was repeated several times to eliminate any trace of lubricant or impurity from the last polishing step. The steel polished surface was etched to elucidate the steel microstructure. For metallographic investigations a Neofot-21 optical microscope was used. The fracture mode and microfractography features of the specimens fracture surfaces after SCC and tensile tests were observed by Carl Zeiss EVO-40XVP scanning electron microscope (SEM).

3. Test results and discussion.

The microstructures of two 17H1S and X60 low-alloyed pipeline steels were examined. The microstructure images of the studied steel samples are shown in Fig. 2. The studied pipeline steels had a microstructure, which consisted predominantly of ferrite and pearlite. The microstructure of 17H1S pipeline steels shows bands of pearlite rich and ferrite rich areas in longitudinal direction as seen in Fig. 2*a, b*. Differences in texture of 17H1S steel depending on directions (transverse and longitudinal) caused by the pipe production technology were observed (Fig. 2*a–d*).

The X60 steel (Fig. 2*e, f*) exhibited a ferrite-pearlite microstructure with the average grain sizes of about 30 μm . The microstructure of X60 steel is significantly finer and more homogeneous than that of 17H1S steel. No microstructure texture of X60 steel was revealed.

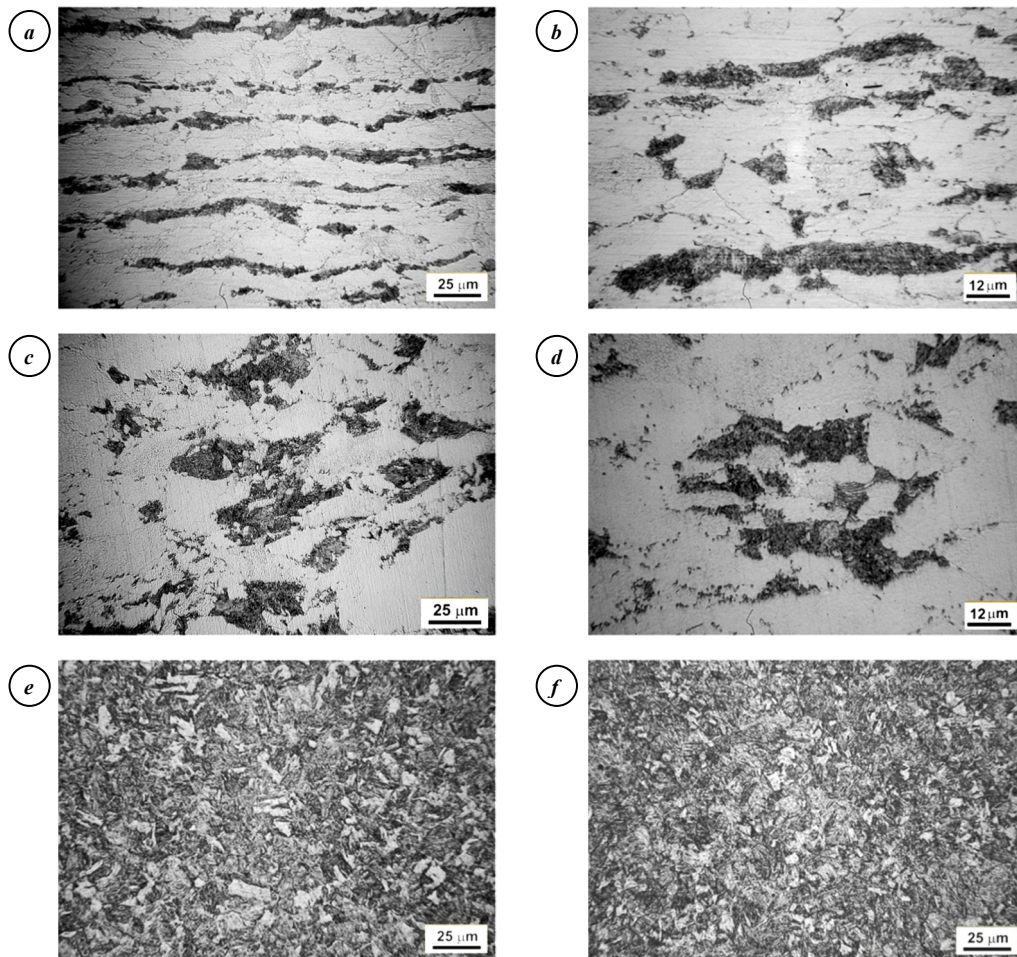


Fig. 2. Optical micrographs of the 17H1S (*a–d*) and X60 (*e, f*) pipeline steel samples in longitudinal (*a, b, e*) and transversal (*c, d, f*) directions.

The potentiodynamic polarization curves for the 17H1S and X60 pipeline steels are shown in Fig. 3. The polarization curves for all studied steels are similar. For both steels, the corrosion potential E_{corr} value is about -0.73 V and the corrosion current density i_{corr} value is ~ 7.4 $\mu\text{A}/\text{cm}^2$. The obtained potentiodynamic curves, as expected in this solution, shows no active-passive transitions in the potential range investigated, only active dissolution. Due to cathodic hydrogen evolution hydrogen can permeate into steel. The driving force for entry into the metal by electrochemical means can be evaluated using the concept of input fugacity as it was proposed by Oriani (1993). If the protective passive film is absent on the steel, the atomic hydrogen can permeate through the

plastic zone of the metal as a function of the input fugacity parameter f_{H_2} . To calculate the input fugacity of hydrogen the overpotential value η for the hydrogen cathodic reaction was determined from the potentiodynamic curves by extrapolating the reversible value of potential by means of the cathodic Tafel slope at the exchange-current density value of iron that equals $i_0 = 10^{-6}$ A/cm². The overpotential value η for given for SSRT studies open circuit condition is 0.08 V. Thus, the hydrogen fugacity parameter f_{H_2} value was $5.65 \cdot 10^2$ atm, calculated by relationship $f_{H_2} = 1 \cdot [e^{(2F/RT) \cdot \eta}]$, where F is Faraday's constant, R – gas universal constant, T – temperature.

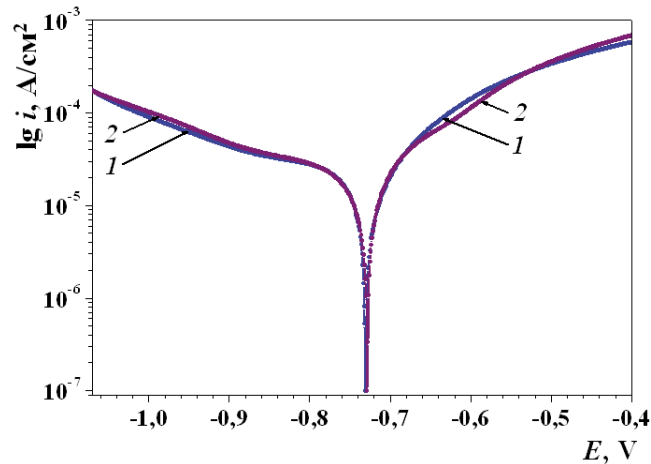


Fig. 3. Potentiodynamic polarization curves for the 17H1S (1) and X60 (2) pipeline steels in NS4 solution saturated with CO₂.

Following the experimental procedure described above, the susceptibility of the 17H1S and X60 pipeline steels to SCC was studied by the SSRT for the as-received and degraded specimens. Average results obtained by tensile tests carried out on studied steels specimens in NS4 test solution saturated with CO₂ under open circuit potential and in air as a reference are illustrated in Table 2. Mechanical properties such as ultimate stress σ_{UTS} , and yield strength σ_Y , reduction in area RA and elongation were calculated from the stress vs. strain curves.

Table 2. Mechanical properties experimentally observed for studied pipeline steels.

Pipeline steel	Steel state	Medium	Ultimate strength σ_{UTS} , MPa	Yield strength σ_Y , MPa	Reduction in area RA, %	Elongation, %
17H1S	As-received	air	470	301	65.9	21.2
	As-received	NS4 saturated with CO ₂	473	304	66.1	21.1
	Degraded	NS4 saturated with CO ₂	467	426	46.4	10.9
X60	As-received	air	592	510	81.9	23.2
	As-received	NS4 saturated with CO ₂	565	489	77.6	21.9
	Degraded	NS4 saturated with CO ₂	610	551	71.3	16.4

According to the data obtained by the SSRT no susceptibility of the 17H1S pipeline steel in the as-received state to SCC in NS4 test solution, saturated CO₂ was revealed. Concerning X60 pipeline steel with higher strength it should be noted that it was characterized by very low sensitivity to SCC in this case. Thus, the presence of the corrosive environment slightly facilitates fracture of the X60 steel specimen in comparison with the test in air: reduction in area and elongation insignificantly decrease.

As it was demonstrated in numerous issues by Tsyryl'nyk et al. (2004), Gabetta et al. (2008) and Nykyforchyn et al. (2010), the long-term exploitation of oil and gas transit pipelines system leads to a noticeable deterioration of the initial mechanical properties, first of all, to a significant decrease of SCC resistance. Taking into account that pipeline serviceability is defined, first of all, by the pipeline steel resistance to brittle fracture, some special

procedures were performed to simulate susceptibility of studied pipeline steels to SCC after their service.

For this purpose some experiments were carried out using specimens after their preliminary loading and artificial aging. The 17H1S steel specimens were subjected to axial loading up to the axial strain of 2.8% with next artificial aging at 250°C for 1 hour. On the basis of the specimens tensile testing it was revealed that they are characterised by ultimate strength σ_{UTS} of 486 MPa, yield strength σ_Y of 375 MPa, reduction in area RA of 63.2% and elongation of 16.1%. As it can be seen from obtained data, the aged 17H1S steel is slightly sensitive to SCC: the corrosive medium slightly decreases the reduction in area parameter.

Then accelerated degradation of pipeline steels with different strength was performed using the experimental procedure described above and enabled in-laboratory simulating of the degradation of the pipeline steel during exploitation under mutual action of hydrogenation and working loading. In all cases, the SSRT on degraded pipeline steels specimens (Table 2) indicated the susceptibility of both investigated steels to SCC in NS4 solution saturated with CO₂ under the open circuit conditions despite the fact that the 17H1S pipeline steel in as-received state revealed no susceptibility to SCC in this medium, and the X60 pipeline steel was characterized by a slight sensitivity to SCC. The degraded 17H1S pipeline steel exhibited the lower resistance to SCC than the degraded X60 pipeline steel as it can be seen from the value of the SCC sensitivity parameter K_{scc} ($K_{scc} = 1 - [RA_{scc} / RA_{air}]$, where RA_{scc} – reduction in area, determined in corrosive environment and RA_{air} – reduction in area, determined in air): $K_{scc} = 0.3$ and 0.13 for the degraded 17H1S and X60 pipeline steels, respectively. So, it can be concluded that the in-laboratory procedure of accelerated degradation of pipeline steels, simulating in-service degradation, increased susceptibility of pipeline steels to SCC in NS4 solution, saturated with CO₂.

Fracture mechanisms of studied pipeline steels specimens during the SSRT in corrosive environment and in air were studied by macro- and micro-fractography analysis, using SEM. Typical SEM photographs of the 17H1S pipeline steel show lower resistance to SCC in the degraded state as presented in Figs. 4–5.

Fig. 4 shows the SEM images of the fracture surfaces of the as-received 17H1S steel specimen after SSRT in air and the degraded 17H1S steel specimen after SSRT in NS4 solution, saturated with CO₂. In general, the fracture mode of the studied material revealed at macro scale is predominantly ductile.

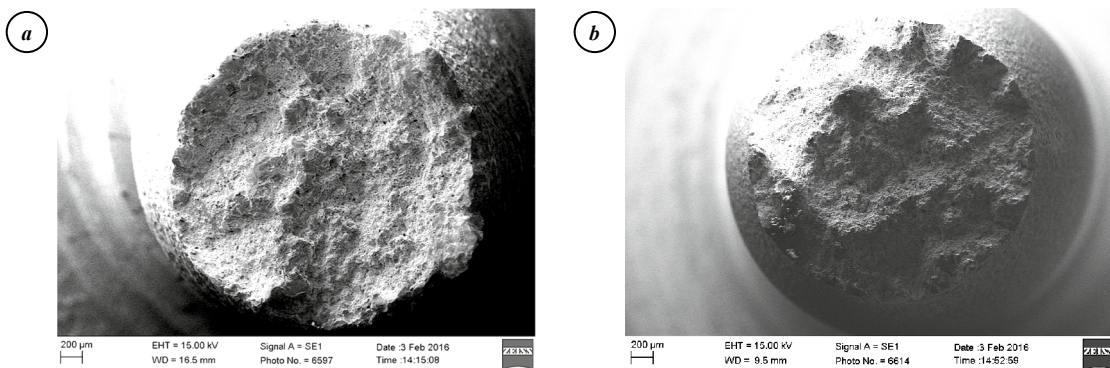


Fig. 4. SEM images, showing the fracture surfaces of the 17H1S steel specimens in the as-received state (a) and after the accelerated degradation (b), SSRT tested in air (a) and in NS4 solution, saturated with CO₂, under open circuit potential (b).

The fracture surfaces of the steel specimen tested in air observed with higher resolution of SEM photographs (Fig. 5a, b) shows that the fracture occurs by the classic scenario: cup and cone fracture with necking. Thus, crack initiation is most likely to occur in the middle of the steel specimen with the subsequent propagation to the surface, which results in the formation of lateral necking. Fig. 5b illustrates dimpled fracture surface observed in the central part of the steel specimen due to microvoid coalescence, resulting in dimpled rupture. In ferritic grains the large voids were mainly formed, and within pearlitic grains – small, which were linked to the laminated cementite. The fracture surface of the specimen lateral surface (Fig. 5a) demonstrates the increasing role of shear processes, that cause the appearance of shallower dimples, disclosing the lower permanent strain ability of these areas along the main loading direction.

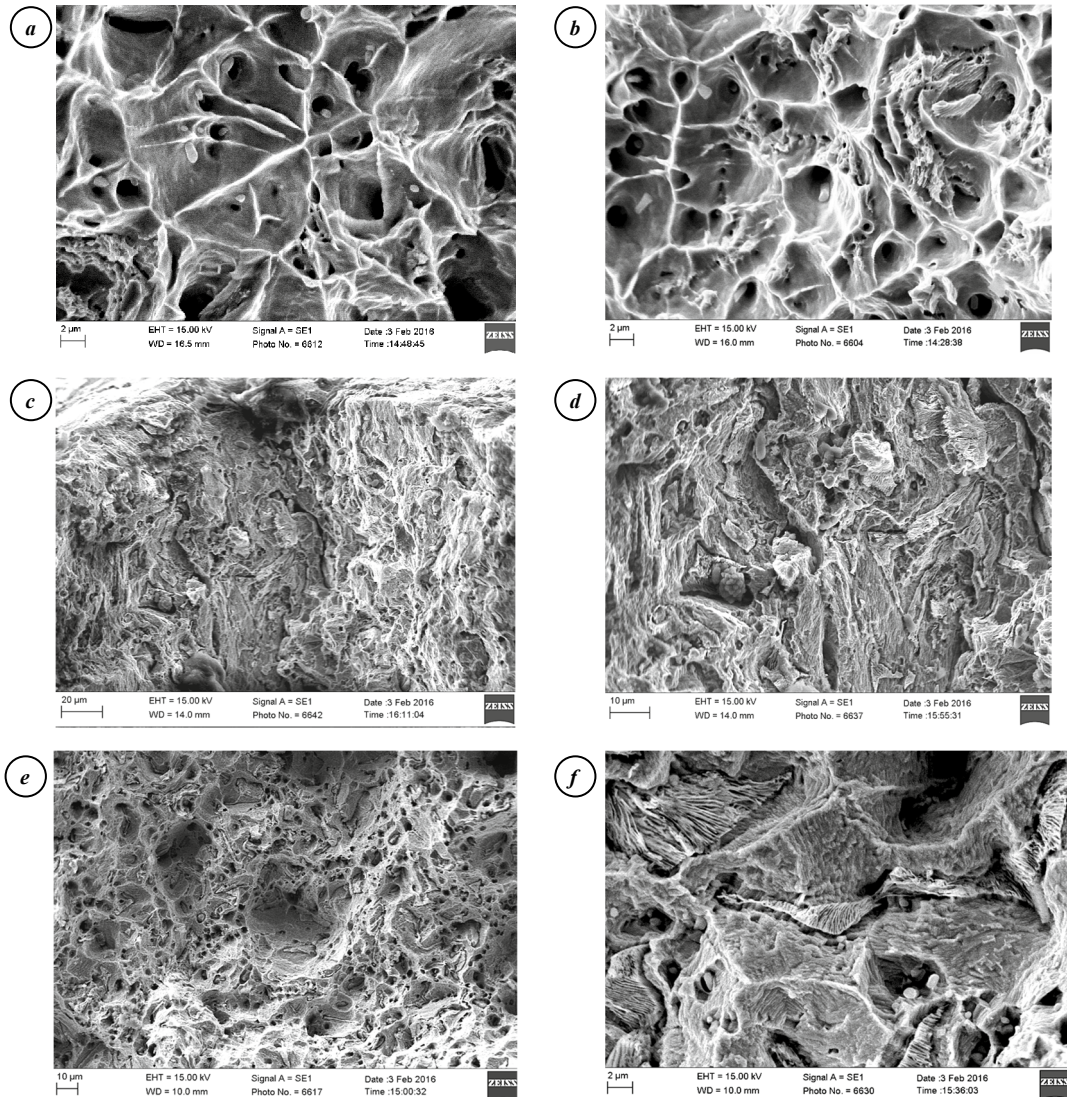


Fig. 5. SEM photographs of the as-received 17H1S steel specimen after SSRT in air (*a, b*) and ones of the degraded 17H1S steel specimen after SSRT in NS4 solution, saturated with CO₂, under open circuit potential (*c–f*), showing fracture features near the side (*a, c, d*) and in the central section (*b, e, f*) of the fracture surface.

Fractographic analysis of the fracture surface of the 17H1S steel specimen subjected to the accelerated degradation and SSRT tested in NS4 solution purged with CO₂ to estimate susceptibility to SCC revealed that the fracture initiated both on local sites of the specimen lateral surface due to SCC (Fig. 5*c, d*), and in the middle of the specimen (Fig. 5*e, f*). The fact that the fracture simultaneously occurred both at the specimen surface (due to SCC), and in the central section of the specimen (due to cracking under the influence of hydrogen absorbed by metal) was confirmed by the presence of the fracture surface area with a net type structure with dimples which was the same as observed at SSRT in air. This fracture area marked off the central fracture surface area and the lateral fracture surface area. And at the same time, the fracture at the lateral surface of the specimen occurred through the formation of narrow transgranular cracks with secondary deep intergranular cracking and the lamination at the interface of ferritic matrix and non-metallic inclusions. The membranes between the cracks were ruptured by the ductile shear fracture mechanism. In the central part of the fracture surface, where the ductile fracture mode was indicated in air (Fig. 5*b*), round fragments with brittle fracture features among the ductile dimpled structure (Fig. 5*e*) were observed

at fracture surfaces of the degraded steel specimens tested in the corrosive environment. There were clearly identified the facets of intergranular cracking with secondary deep cracking along the ferritic grains interfaces (Fig. 5f) at higher resolution of SEM photograph. In pearlitic grains the interfaces of ferritic matrix and cementite plates were distinguished on the fracture surface, which could be due to cracking along the interfaces. Brittle transgranular elements in the ductile fracture mode were earlier observed in the central section of the fracture surfaces of pre-hydrogenated smooth specimens of above 20 years exploited steam pipelines tested in air as it was demonstrated by Nykyforchyn et al. (2007) and Krechkovs'ka (2016). These elements were caused by local facilitation of brittle fracture of metal under the influence of hydrogen being accumulated in damages formed during long-term exploitation. In studied case hydrogen influenced the formation of damages during the accelerated degradation of the pipeline steel. Grain boundaries were favourable trapping sites for the accumulation of hydrogen, so intergranular cracking within the brittle elements could be associated with this phenomenon. These results are confirmed by data of Voloshyn et al. (2015), demonstrating that the basic mechanism of both initiation, and propagation of SCC in near-neutral-pH solution is hydrogen embrittlement of pipeline steel.

4. Summary

The developed procedure of the accelerated degradation, consisting in consistently subjecting the steel specimens to electrolytic hydrogen charging, axial loading up and artificial aging, proved to be reliable and useful for laboratory simulation of in-service degradation of pipeline steels of different strength. The results of the SSRT carried out on the in-laboratory degraded 17H1S and X60 pipeline steels to evaluate the SCC susceptibility demonstrated that specimens tested in the NS4 solution saturated with CO₂ under open circuit potential and room temperature presented susceptibility to SCC, reflected in the degradation of mechanical properties, whereas high resistance of the as-received pipeline steels to SCC was detected. The as-received steel specimens tested in air exhibited a ductile type of fracture. The structure of the degraded steel specimens tested in corrosive solution showed fragments with brittle fracture features among the ductile dimpled structure. The degraded X60 steel showed higher resistance to SCC in comparison with the degraded 17H1S steel. Fractographic observation confirmed that hydrogen embrittlement of pipeline steels was caused by permeated hydrogen inside them.

Acknowledgements

The research has been supported by the NATO in the Science for Peace and Security Programme under the Project G5055.

References

- Elboujdaini, M., Wang, Y., Revie, R., 2000. Initiation of stress corrosion cracking on X65 line pipe steels in near-neutral pH environment. Proceedings of the International Pipeline Conference ASME 2000, Calgary, Canada.
- Gabetta, G., Nykyforchyn, H., Lunarska, E., Zonta, P. P., Tsyrlunyk, O. T., Nikiforov, K., Hredil, M. I., Petryna, D. Yu., Vuherer T., 2008. In-service degradation of gas trunk pipeline X52 steel. *Materials Science* 44, No. 1, 88–99.
- Integrity of Pipelines Transporting Hydrocarbons – Corrosion, Mechanisms, Control, and Management, 2011. In “*NATO Science for Peace and Security. Series C: Environmental Security*”. In: Bolzon, G., Boukharouba, T., Gabetta, G., Elboujdaini, M., Mellas, M. (Eds.). Springer Science + Business Media B.V., 322 p.
- Krechkovs'ka, H. V., 2016. Fractographic features of hydrogen transport mechanisms in structural steels. *Materials Science* 51, No. 4 (in press).
- Lu, B., Luo, J., 2006. Relationship between yield strength and near-neutral pH stress corrosion cracking resistance of pipeline steels - An effect of microstructure. *Corrosion* 62, No. 2, 129–140.
- Nykyforchyn, H. M., Student, O. Z., Markov, A. D., 2007. Abnormal behavior of high-temperature degradation of the weld metal of low-alloy steel welded joints. *Materials Science* 43, No. 1, 77–84.
- Nykyforchyn, H., Lunarska, E., Tsyrlunyk, O. T., Nikiforov, K., Genarro, M. E. & Gabetta, G., 2010. Environmentally assisted in-bulk steel degradation of long term service gas trunkline. *Engineering Failure Analysis*, 17(3), 624–632.
- Oriani, R. A., 1993. The Physical and Metallurgical Aspects of Hydrogen in Metals. Fourth International Conference on Cold Fusion. Lahaina, Maui.
- Tsyrlunyk O. T., Nykyforchyn, H. M., Zvirko, O. I., Petryna, D. Yu., 2004. Embrittlement of the steel of an oil-trunk pipeline. *Materials Science* 40, No. 2, 302–304.
- Voloshyn, V. A., Zvirko, O. I., Sydor, P. Ya., 2015. Influence of the compositions of neutral soil media on the corrosion cracking of pipe steel. *Materials Science* 50, No. 5, 671–675.